Responses to Reviewer #2

Thank you very much for your comments and suggestions on our paper. They were very useful in revising the manuscript. The revised Table and Figures are attached at the end of this text.

Reply to specific comments:

Abstract: In response to the reviewer's comment, we have spelled out the use of FLEXPART after the second sentence. As the reviewer mentioned, "gradual decrease" is inconsistent with "no trend" period. Consequently, the 3rd sentence of the original manuscript in Abstract has been changed to "To investigate the relationship between the East Asian emissions and the short-term variations in the atmospheric mixing ratios, we use FLEXPART Lagrangian particle dispersion model (LPDM). The observed ratios $\Delta CH_4/\Delta CO_2$ and $\Delta CO/\Delta CO_2$ both show an overall gradual decrease over the study period due to a recent rapid increase in fossil fuel consumption in China. We note, however, that the decreasing rates of $\Delta CH_4/\Delta CO_2$ and $\Delta CO/\Delta CO_2$ show gradual decrease and increase, respectively, during the entire observation periods used in this study."

p. 22894, l. 25: "the second most important greenhouse gas" has been changed to "the second most important anthropogenic greenhouse gas".

p. 22895, l. 4: "Resent" has been changed to "Recent".

p. 22895, l. 10: As the reviewer suggested, soil absorption and reaction with Cl and O^1D radials in the stratosphere are important sink for CH_4. We have changed the relevant part "the destruction by hydroxyl radical (OH) in the atmosphere" to "loss processes that include soil absorption and chemical reactions with atmospheric hydroxyl radical (OH) and stratospheric $O(^1D)$ and Cl atoms".

p. 22895, l. 16: Following the reviewer's suggestion, we have changed "other greenhouse gases" to "other species".

p. 22895, l. 18: Yes, CO always acts as a precursor of tropospheric O_3 under the condition that an adequate supply of NO is available. Thus, following the reviewer's suggestion, "CO could act as" has been changed to "CO acts as".

p. 22895, l. 22: "pollutants" has been changed to "air pollutants".

p. 22895, l. 25: In response to the reviewer's comment, we have added "(e.g. Emission Database for Global Atmospheric Research (EDGAR) v4.2 (EC-JRC/PBL, 2011); Carbon Dioxide Information Analysis Center (CDIAC) (Boden et al., 2011); Regional Emission inventory in ASia (REAS) v2.1 (Kurokawa et al., 2013))" after the 1st sentence of the 3rd paragraph in Introduction to cited EDGAR v4.2, REAS v2.1, and CDIAC.

p. 22896, l. 2: As the reviewer suggested, much of CH_4 increase in China is thought to be attributed to the fugitive emission from solid fuel or coal mining. To be more specific, "fossil fuels" has been changed to "coal mining".

p. 22896, l. 5: In response to the reviewer's comment, we have added the clause "because those emissions related to complete combustion are generally well estimated while the emissions related to incomplete combustion and agricultural activities are poorly constrained (Kurokawa et al. 2013)" after the relevant sentence of the 3rd paragraph in Introduction.

p. 22896, l. 10-13: Following the reviewer's suggestion, we have combined the two sentences into "Downward from the source regions, a synoptic-scale variation (SSV) in the mixing ratio of one chemical species is usually associated with SSVs of other species that have similar regional emission distributions and atmospheric lifetime characteristics."

p. 22896, l. 15: "known" has been deleted.

p. 22897, l. 8: We consider that the shorter-term variations, i.e., 24-hour variations based on hourly data, may reflect more directly the regional emissions because the contribution of large-scale air mass mixing to the variations increases with data period. To state this clearly, we have added a sentence, "Here we examine 24-hour variations based on the hourly data because shorter-term variations are likely to reflect more directly the regional emissions from the East Asian countries." after the 1st sentence of the last paragraph in Introduction.

p. 22897, l. 19: "only an outline description" has been changed to "only a brief description".

p. 22900, l. 22-24: We agree the reviewer's comment that the $\Delta CO/\Delta CH_4$ seasonality is mainly attributed to the seasonality in the air mass transport and the regional contrast of the CO/CH_4 emission ratio. To explain the air mass transport during summer, we have added an average footprint for the measurements at HAT during the summer period (May to September) in Figure S4. Additionally, faster destruction of CO in the summer and seasonality in the CH_4 and CO emissions may also contribute to the $\Delta CO/\Delta CH_4$ seasonality. Consequently, we have changed the 4th and 5th sentences of the relevant paragraph (3rd paragraph in Section 3) "We also note that …in the average $\Delta CO/\Delta CH_4$ slope" to "We also note that the seasonal variation in the average $\Delta CO/\Delta CH_4$ slope may be attributable mainly to the seasonality in the air mass transport. During the summer, air masses arriving at HAT are predominantly transported from the Pacific region and the contributions of the South East Asian emissions show a relative increase. (Figure S4 shows the average footprint, which is discussed in Section 4.1, during the summer period (May to September)). Thus the average $\Delta CO/\Delta CH_4$ slope is low in summer because the CO/CH_4 emission ratios for the South East Asian countries are lower than those for China, Japan and Korea (e.g. Kurokawa et al., 2013). However, it is possible that the seasonality in the emissions from East Asia, the maximum CH_4 emissions in summer (Yan et al.,, 2003) and the maximum CO emissions in winter (Streets et al., 2003; Zhang et al., 2009), and the significantly faster CO reaction with OH in summer could partially contribute to the seasonality in the average $\Delta CO/\Delta CH_4$ slope."

p. 22901, l. 8: The 5-month period is shorter than the 6-month period used for Tohjima et al. (2010). To state this clearly, we have added "The 5-month winter period used for

this study is shorter than the 6-month winter period (November to April) used in a previous study by Tohjima et al. (2010).” to the end of the last paragraph in Section 3.

p. 22903, l. 8 (maybe l. 24-25?): Although we have not been able to conduct any pattern analysis, we have compared the spatial distributions of the CO_2, CH_4, and CO flux maps prepared in the revised manuscript (EDGAR v4.2, REAS v2.1, ODIAC, and Patra et al., 2009). The emission maps are depicted in Figure S5. As is shown in the figures, the strong emissions are primarily confined to the land areas in the southern part of North China, East China, the Korean Peninsula, and Japan in any flux maps. Therefore, we consider that the CO_2, CH_4, and CO fluxes have roughly similar spatial distributions within EFA. To state this clearly, we have added the sentences “To examine the robustness of this assumption, we compare the flux maps prepared in Section 4.2 (see Figure S5). Since the strong emissions, primarily confined to the land areas, are generally distributed in the southern part of North China, East China, the Korean Peninsula, and Japan, we are confident that the spatial distributions of the CO_2, CH_4, and CO fluxes within EFA are roughly similar to each other.” to the end of the 2nd paragraph in Section 4.3.

p. 22904, l. 19-20: We analyzed the histogram of the correlation slopes of the simulated $\Delta CH_4/\Delta CO_2$ and $\Delta CO/\Delta CO_2$, which are discussed in Section 5.2, and found that a similar narrowing of the histogram occurs. In this simulation, the national emissions and emission distributions of the fossil fuel-derived CO_2 are changed according to CDIAC and EDGAR v4.2, respectively. To examine the contribution of the changes in the emission distribution to the narrowing of the histogram, we have repeated the above analysis with the CO_2 emission distribution fixed to that for 1998. The results show the similar narrowing of the histogram (shown in Figure S6), suggesting that the emission increase is main contributor to the narrowing. To state this, we have added the following sentences “The histograms of the correlation slopes of the simulated $\Delta CH_4/\Delta CO_2$ and $\Delta CO/\Delta CO_2$ (see Section 5.2) show similar temporal changes as in the observation: the distributions become narrow in association with the increase in the fossil-fuel derived CO_2 emissions in China (see Fig. S6, in which the histogram of the simulated $\Delta CH_4/\Delta CO_2$ for 1998/1999 and 2009/2010 and $\Delta CO/\Delta CO_2$ for 2001/2002 and 2009/2010 are depicted). Note that the histograms of the simulated $\Delta CH_4/\Delta CO_2$ and $\Delta CO/\Delta CO_2$ driven by the 1998 fossil CO_2 emission map show a similar temporal change in the distribution, suggesting that the contribution of the change in the emission distribution is relatively small.” to the end of the first paragraph in Section 5.1.

p. 22906, l. 2: The CH_4 and CO emission maps are fixed to those for 2007, which is mentioned in Section 4.2 and in the last sentence of the 2nd paragraph in Section 5.2.

p. 22906, l. 13: In this study, we have been able to use the 5-year (2006-2010) concentration footprints computed by FLEXPART, as is mentioned Section 4.3. Therefore, the relationship between the regional emissions and the correlation slopes are computed by using the 5-year concentration footprints. The variability in of the correlation slopes caused by the year-to-year variation in the meteorological conditions is estimated from the variability in the simulation based on the 5-year concentration footprints. To state this clearly, we have added “Since the simulated correlation slopes from the annual CO_2 emissions are based on a 5-year (2006-2010) concentration footprint calculated by FLEXPART, the annual emission estimates don’t reflect the meteorological field of the corresponding years. The influence of the year-to-year

variation in the meteorological condition on the simulated correlation slope is therefore part of the variability of the 5-year simulation." after the last sentence of the 1st paragraph in Section 5.3.

p. 22907, l. 7: To remove ambiguity, we have changed the relevant sentence "There results seem to …at HAT" to "These results seem to suggest that the emissions from EFA outside China contribute little to the observed changes in the average correlation slopes at HAT and the emissions from the Chinese part of the EFA can be robustly estimated by both scenarios".

p. 22907, l. 16: "in Fig. 7 as open orange squares" has been changed to "in Fig. 7c as black open squares".

p. 22908, l. 15: Similarly, Reviewer #1 also suggested carrying out more discussions on the CH_4 emission estimates in Section 5.4.1. In response to the reviewers' comments, we have added the comparisons of our CH_4 estimate with the results from REAS v2.1, the TranCom-CH_4 experiment (Patra et al., 2011), and the recent inversion study using satellite and ground observations (Bergamaschi et al., 2013). Consequently, Section 5.4.1 has been changed to "Bottom-up estimates of the CH_4 emission from Chinese anthropogenic sources without the rice fields taken from the inventory databases EDGAR v4.2, REAS v1.1 (Ohara et al., 2007, http://www.jamstec.go.jp/frcgc/research/p3/emission.htm) and REAS v2.1 are plotted for comparison with our results in Fig. 9. The EDGAR v4.2 emission estimates show good agreement with our estimates for the period 1998 to 2002. However, after 2002 the EDGAR v4.2 data show a much faster increase of 3.1 ± 0.1 $TgCH_4\ yr^{-2}$ (2002-2008), which is about 3 times larger than our estimates of 1.1 ± 0.2 $TgCH_4\ yr^{-2}$ (2002-2010). The REAS v2.1 estimates, being higher than our estimates, also show a faster increase of 3.6 ± 0.2 $TgCH_4\ yr^{-2}$ (2000-2008). About 70% and 90% of the increases in the Chinese emissions in the EDGAR v4.2 and REAS v2.1 estimates, respectively, are attributed to the emissions related to coal mining (fugitive emissions from solid fuels), and occurs mostly within EFA. Note that the REAS v1.1 estimates are lower than our estimates and the differences from the REAS v2.1 estimate for 2000 are attributed to the fugitive emissions from fossil fuels (73%) and the emissions from land disposal of solid waste (24%).

The possibility that the CH_4 emissions in the EDGAR v4.2 inventory are overestimated was also suggested by the following model studies. In a chemistry-transport model intercomparison experiment of CH_4 (TransCom-CH_4), the forward simulations of atmospheric CH_4 were conducted using several transport models and various sets of surface CH_4 emission scenarios (Patra et al., 2011). The forward CH_4 simulation based on the EDGAR v4.0 emissions, which are almost same as the EDGAR v4.2 emissions, shows a significantly faster growth rate during 2003-2007 than the observations. The Chinese emission increase contributes nearly 40% to the global CH_4 emission increase in the EDGAR inventory. Recently, Bergamaschi et al. (2013) estimated global CH_4 emissions during the 2000s based on an inverse modeling constrained by atmospheric CH_4 data from the global air sampling network and satellite sensor. The inversion result shows a significant increase in the anthropogenic CH_4 emissions from China but a smaller increase than that indicated by the EDGAR inventory. The increasing rate of 1.1 ± 0.3 $TgCH_4\ yr^{-2}$ estimated by Bergamaschi et al. (2013) for the period of 2000-2010 is in excellent agreement with our estimation.

Therefore, we suspect that the EDGAR v4.2 and REAS v2.1 inventories are overestimating the recent increase in the CH_4 emissions related to the coal mining."

p. 22908, l. 16: Both EDGAR v4.2 and REAS v2.1 are overestimating the CH_4 emissions from the coal mining activity in China. We state this clearly in the revised manuscript.

p. 22909, l. 17: We agree with the reviewer's comment that the discrepancy of CO emission estimates between EDGAR and other studies could be attributed to the secondary CO production (oxidation products from VOCs), of which values are included in the top-down estimates but not explicitly included in EDGAR inventories. Therefore, we have changed the 2nd paragraph of Section 5.4.2 to "The top-down estimates including ours reflect not only the primary CO emissions but also the secondary CO production from the oxidation of NMVOC. However, we consider the contribution of the CH_4 oxidation to the top-down estimates of CO emissions based on the atmospheric observations in the downwind regions from China to be negligible because of the much longer life time of atmospheric CH_4 (about 10 yr, e.g. Patra et al., 2011) compared to its transit time. It is to be noted that the EDGAR database reports only the primary CO emissions. Duncan et al. (2007) estimated that the oxidation of NMVOC contributes nearly 50% of the total primary CO emissions to the global CO emission. If this ratio is valid and can be applied to the EDGAR estimate for China, then the resulting net CO emissions with both primary and secondary sources can be applied to our top-down estimates. In addition, our winter emission estimates would of course be biased if the CO emission has a noticeable seasonality. For example, using monthly data for power generation and industry, as well as residential energy consumption, Zhang et al. (2009) developed a dataset of monthly CO emissions from China. The result shows a significant seasonality, with 17% larger average monthly emission for our 5-month winter than for an entire year. If in fact there is a strong seasonal variation in the CO emission, then our winter estimate needs to be reduced by 17%, which also brings our estimate close to the EDGAR v4.2 estimate. Above discussion points to the importance of correct evaluation of the secondary CO emissions when comparing top-down and bottom-up emission estimates. Note that the REAS v2.1 estimates, in which the secondary CO emissions are not explicitly included, agree well with the top-down estimate. Kurokawa et al. (2013) attribute the differences in the CO emissions between REAS v2.1 and EDGAR v4.2 to the emission factors used in the estimations; the emission factors for REAS v2.1 might implicitly include the secondary productions."

Following this change, we have added the sentence "However, this discrepancy may be attributed to the secondary CO production derived from the atmospheric oxidation of NMVOC, which is not included in the EDGAR bottom-up estimation." to the end of the last paragraph in Conclusion.

Figure 1.: Following the reviewer's suggestion, we have removed USA line from Fig. 1.

Figure 4c.: "ppb/ppm" of y-axis units has been changed to "ppb/ppb".

Figure 5. caption: "foot print" has been changed to "footprint".

Figure 6. caption: "slops" has been changed to "slopes".

Figure 7c.: To explain these open squares, we have added the sentence “The black open squares in **Fig. 7c** represent the $\Delta CO/\Delta CH_4$ slopes based on the optimized CH_4 and CO emissions from China within EFA (see text).” in the caption. In response to the reviewer’s comment, we have redrawn the figure in which the data for “Obs.” are plotted as same red symbols.

Figure 9.: “READ” has been changed to “REAS”.

Revised Table and Figures are shown below:

Table 1. Summary of the estimated CH_4 and CO emissions from China[a]

Year	Fossil fuel CO_2[b]	CH_4[c, d]	CO[d]
1997/1998	0.93	38.4 ± 6.8	
1998/1999	0.91	40.5 ± 7.0	134 ± 32
1999/2000	0.92	37.3 ± 6.6	149 ± 34
2000/2001	0.94	39.4 ± 6.8	140 ± 35
2001/2002	0.98	39.1 ± 6.9	153 ± 36
2002/2003	1.12	37.3 ± 6.4	158 ± 36
2003/2004	1.34	40.7 ± 7.2	179 ± 42
2004/2005	1.51	39.4 ± 6.7	182 ± 42
2005/2006	1.66	44.0 ± 7.4	176 ± 40
2006/2007	1.80	43.3 ± 7.3	169 ± 38
2007/2008	1.88	44.7 ± 7.6	181 ± 41
2008/2009	1.98	46.5 ± 7.9	150 ± 33
2009/2010	2.14	45.8 ± 7.9	159 ± 36

[a]Values for CO_2 are given in PgC yr^{-1}, for CH_4 in $TgCH_4$ yr^{-1}, and for CO in TgCO yr^{-1}.
[b]Fossil CO_2 emissions are taken from the CDIAC database. Each value is the average of the emissions for the consecutive two years described in the first column. The uncertainty is assumed to be 15%, which is the lower limit of the estimation of Gregg et al. (2008).
[c]Values represent the emissions from non-seasonal CH_4 sources (see text).
[d]Uncertainties are calculated from the uncertainties of the fossil fuel-derived CO_2 emissions in China, of the observed correlation slopes including the influence of the correlation coefficient criteria selection, and of the simulated correlation slopes including the influence of the uncertain emission distributions used in the simulation (see text).

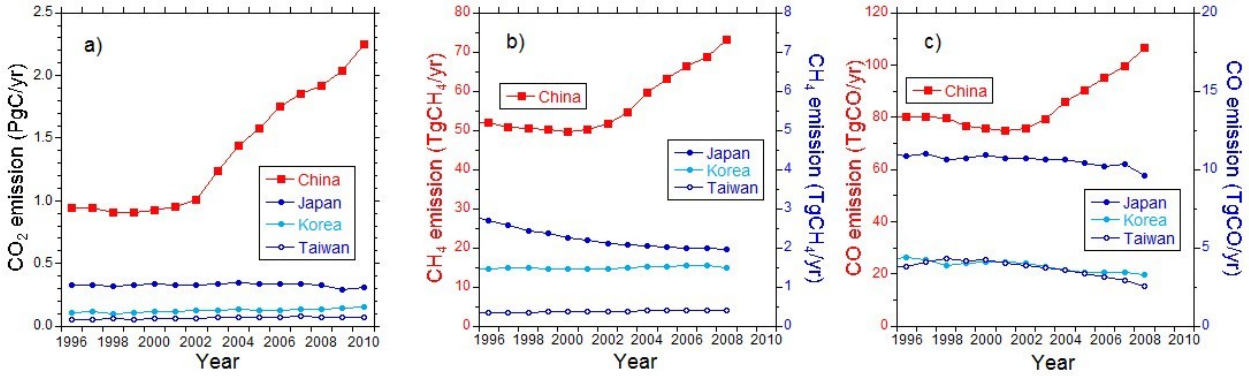

Fig. 1. Temporal changes in the estimated emissions of (a) fossil fuel-derived CO_2, (b) CH_4, and (c) CO from China, Japan, Korea, and Taiwan. The CO_2 emissions are taken from the CDIAC database. CH_4 and CO emissions are taken from EDGAR v4.2. CH_4 and CO emissions from Japan, Korea and Taiwan are plotted against the right-Y axis.

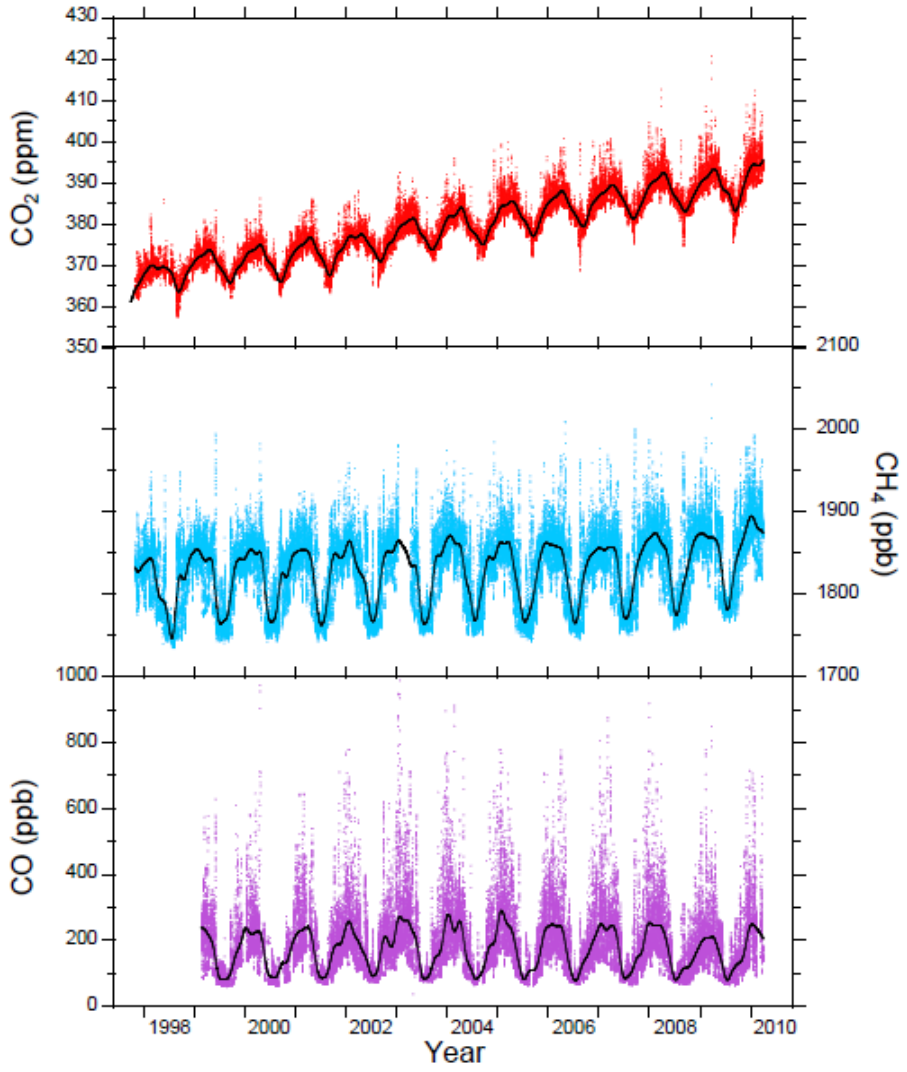

Fig. 2. Time series of atmospheric (top) CO_2, (middle) CH_4, and (bottom) CO mixing ratios observed at HAT. Each dot represents hourly average. Black lines represent the smooth curve fits to the data.

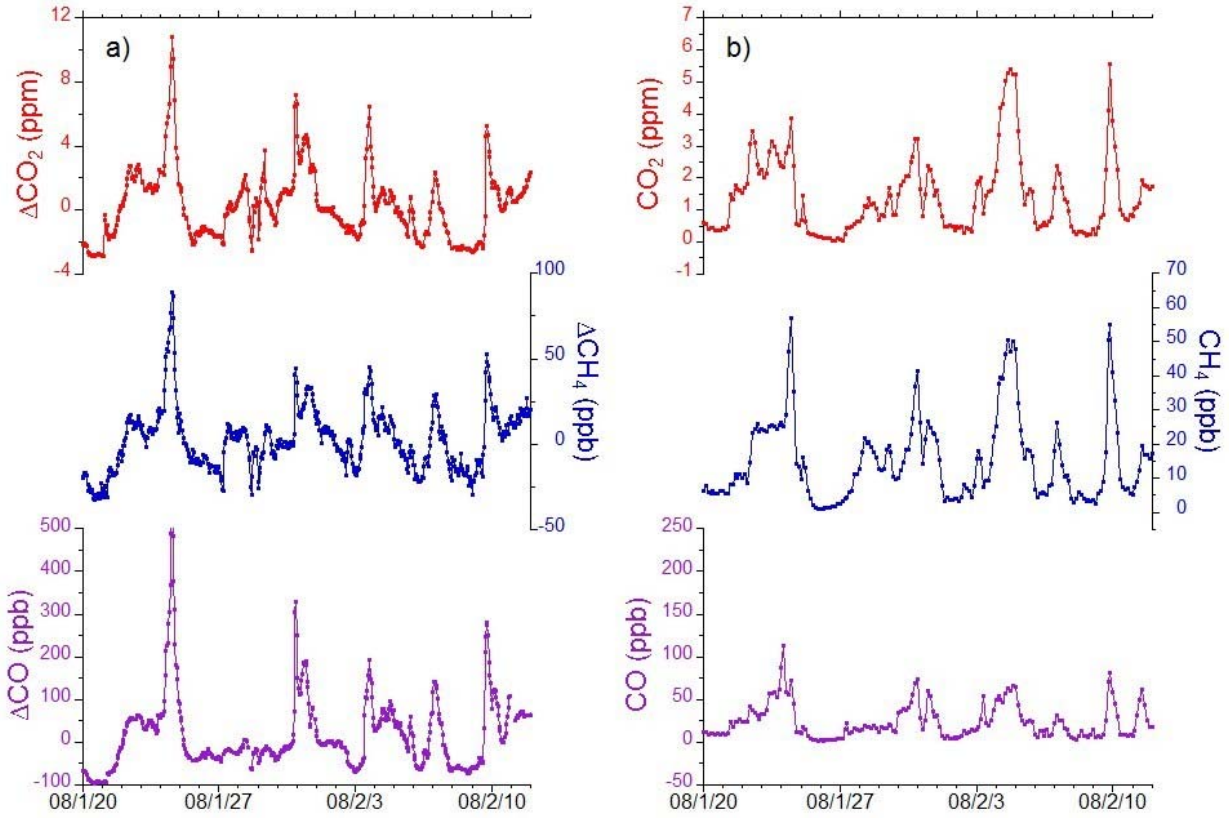

Fig. 3. Synoptic scale variations in hourly (top) CO_2, (middle) CH_4, and (bottom) CO based on (a) the observation and (b) the model simulation for the period from January 20 to February 12, 2008. The range of the y-axis for the simulation plot for each chemical species is half of that for the corresponding observation plot.

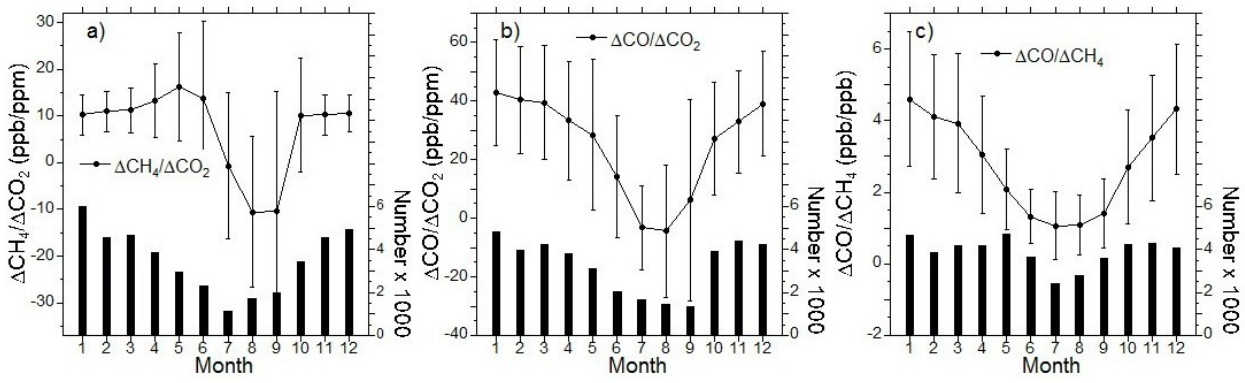

Fig. 4. Average seasonal variation of (a) $\Delta CH_4/\Delta CO_2$, (b) $\Delta CO/\Delta CO_2$, and (c) $\Delta CO/\Delta CH_4$ slopes observed at HAT. The error bars represent the standard deviations from the monthly averages. The vertical bars represent the data number.

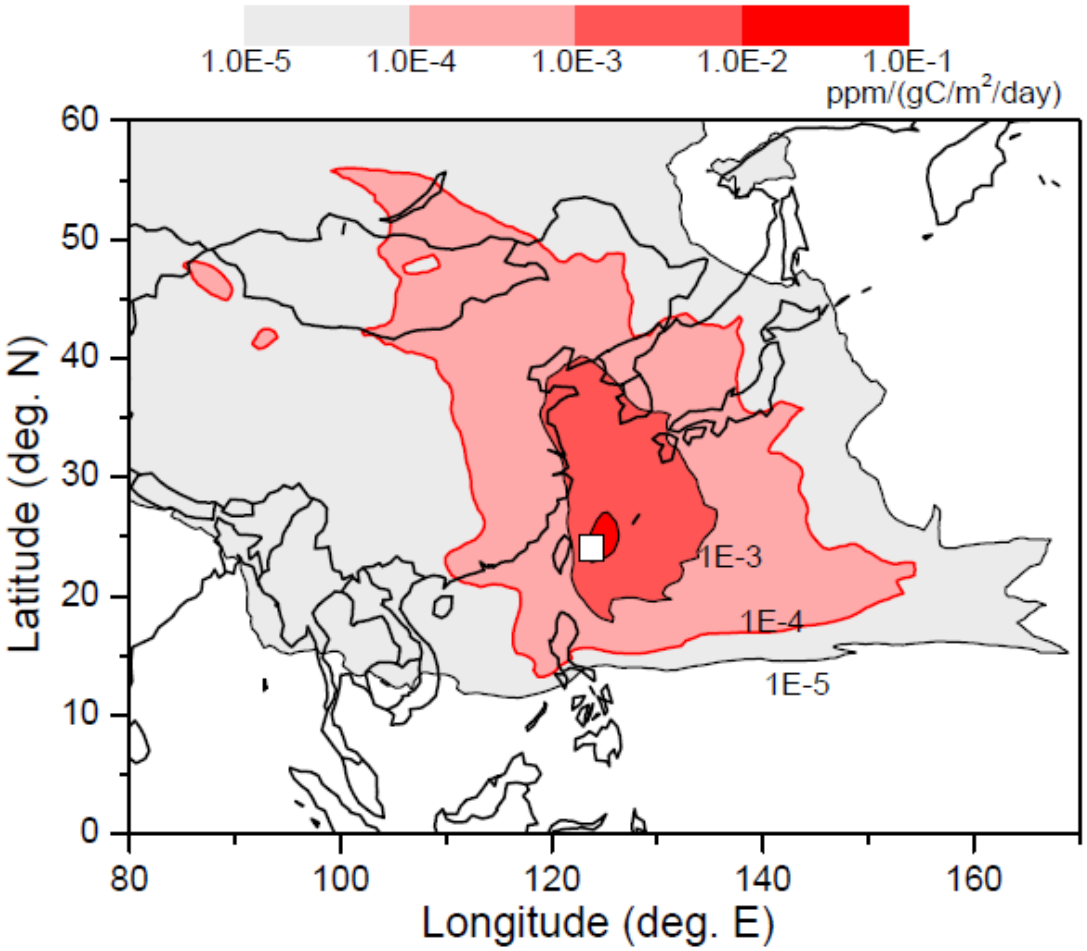

Fig. 5. Average footprint (ppm (gC m^{-2} day^{-1})$^{-1}$) for the measurements at HAT during the winter period (November to March). Meteorological data for 2006-2010 are used for the calculation. The location of HAT is indicated by the square. The area surrounded by the red thick contour lines of 1×10^{-4} ppm (gC m^{-2} day^{-1})$^{-1}$ is defined as an effective footprint area (EFA).

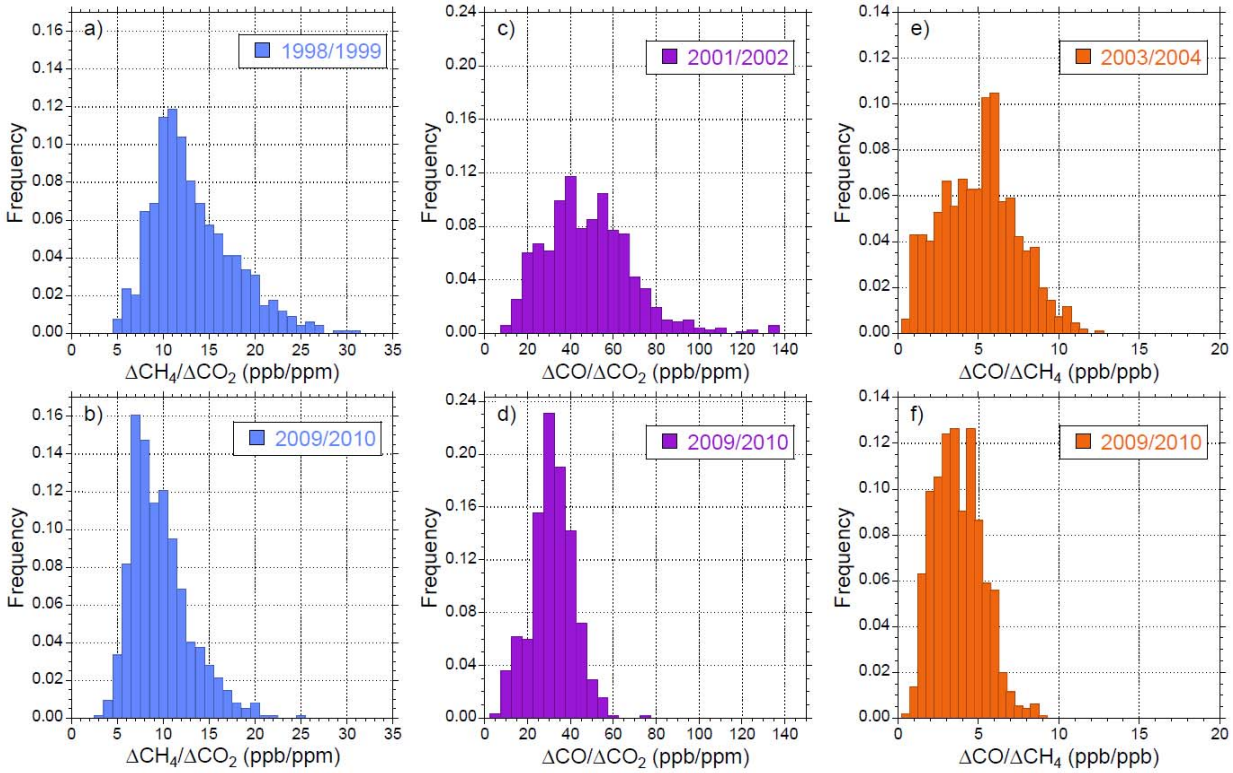

Fig. 6. Histograms of the correlation slopes of (a, b) $\Delta CH_4/\Delta CO_2$, (c, d) $\Delta CO/\Delta CO_2$, and (e, f) $\Delta CO/\Delta CH_4$ for the selected two periods. The correlation slopes all meet the selection criteria (see text).

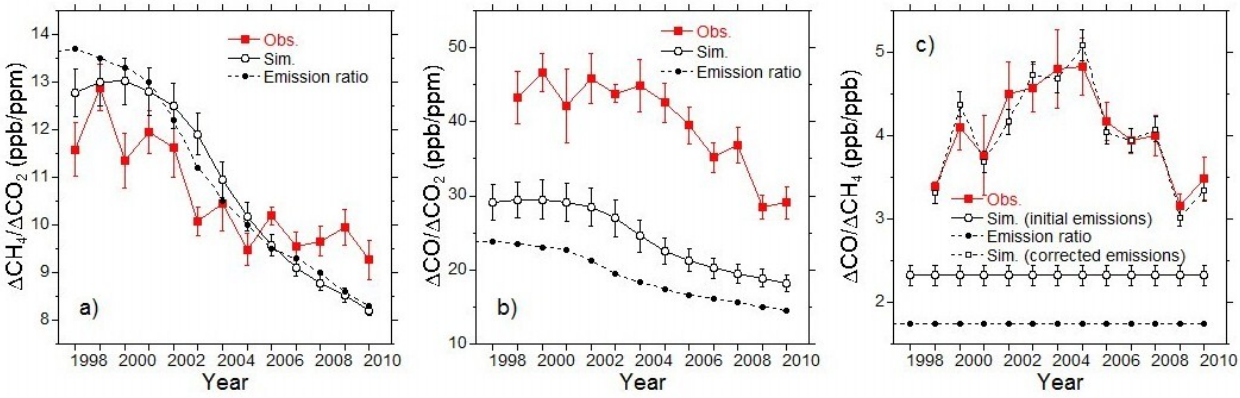

Fig. 7. Temporal changes in the winter average correlation slopes of (a) $\Delta CH_4/\Delta CO_2$, (b) $\Delta CO/\Delta CO_2$, and (c) $\Delta CO/\Delta CH_4$. The red closed squares represent the observation and the open circles represent the simulation. The error bars represent the standard errors. The ratios of the emissions within EFA are also depicted as closed circles. The black open squares in **Fig. 7c** represent the $\Delta CO/\Delta CH_4$ slopes based on the optimized CH_4 and CO emissions from China within EFA (see text).

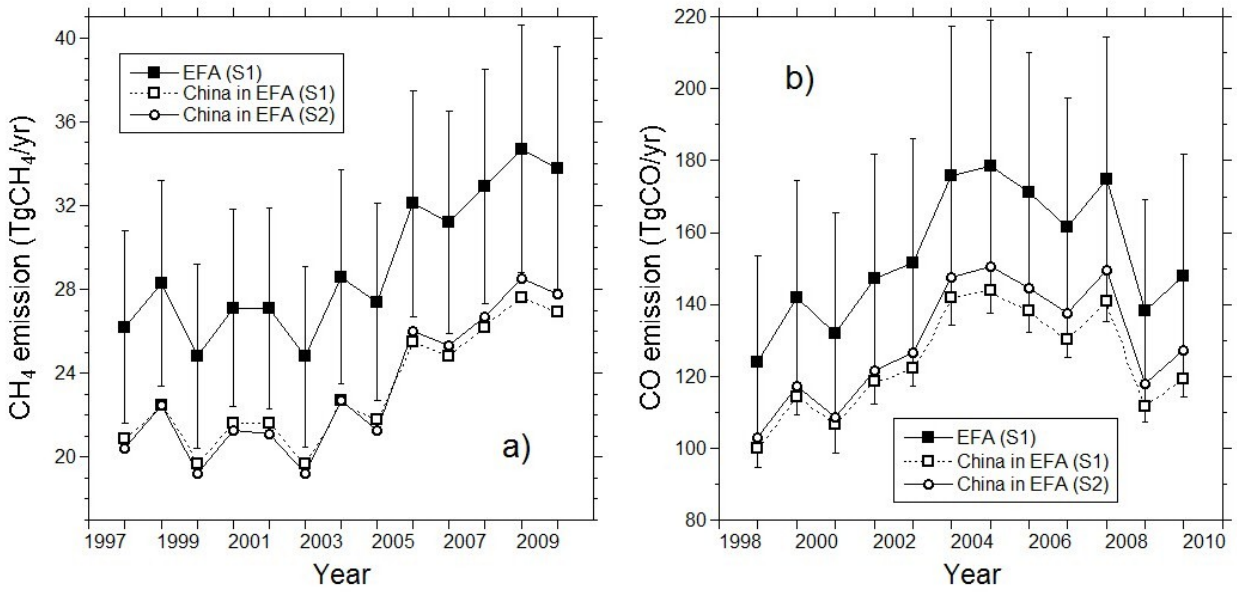

Fig. 8. Temporal changes in the estimated (a) CH_4 and (b) CO emissions from EFA. The emissions from EFA for S1 are depicted by closed squares with uncertainties. The emissions from China in EFA are depicted for S1 by open squares and for S2 by open circles (see text).

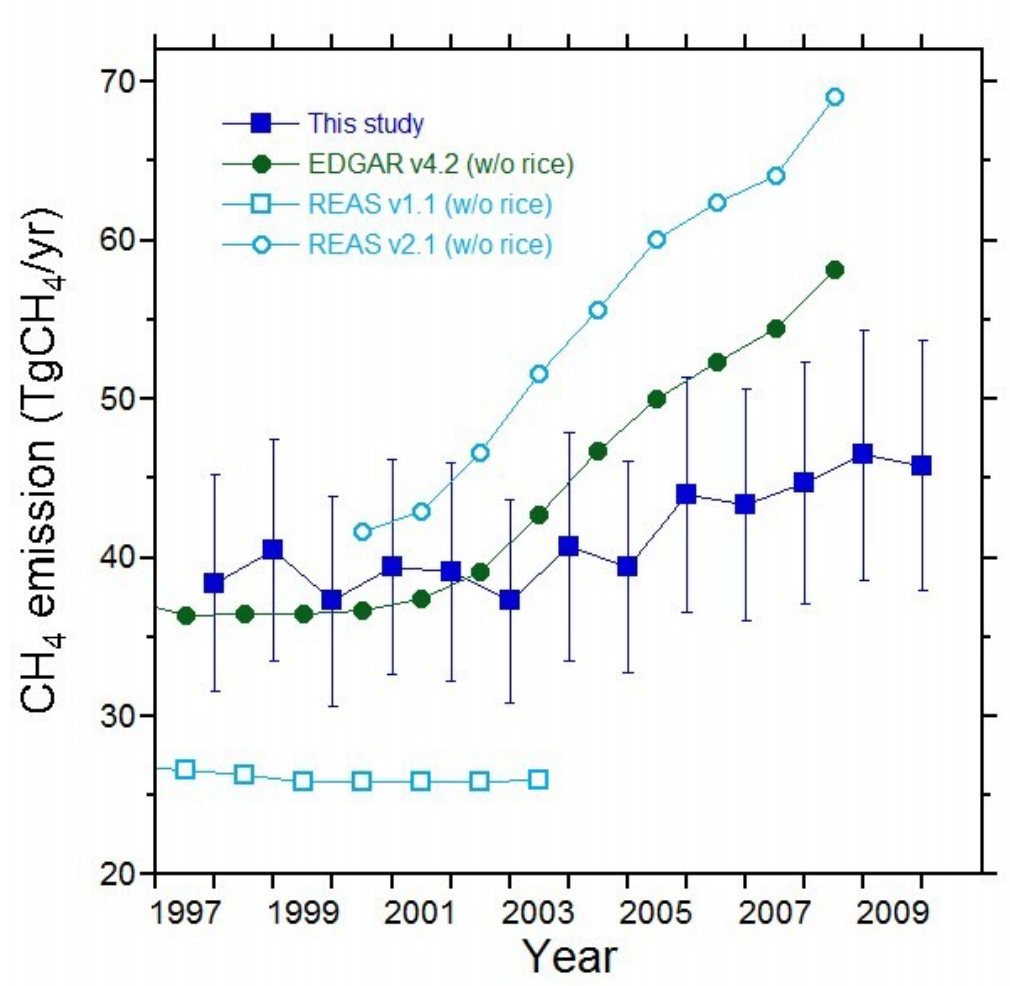

Fig. 9. Comparison of estimated non-seasonal CH_4 emissions from China. The values are expressed as annual emissions. Closed blue squares are the estimated emissions of this study. Green circles, light blue squares, and light blue circles represent the CH_4 emissions from anthropogenic sources (excluding rice fields) in China based on the emission inventories from EDGAR v4.2 (http://edgar.jrc.ec.europa.eu/), REAS v1.1 (Ohara et al., 2007) and REAS v2.1 (Kurokawa et al., 2013), respectively.

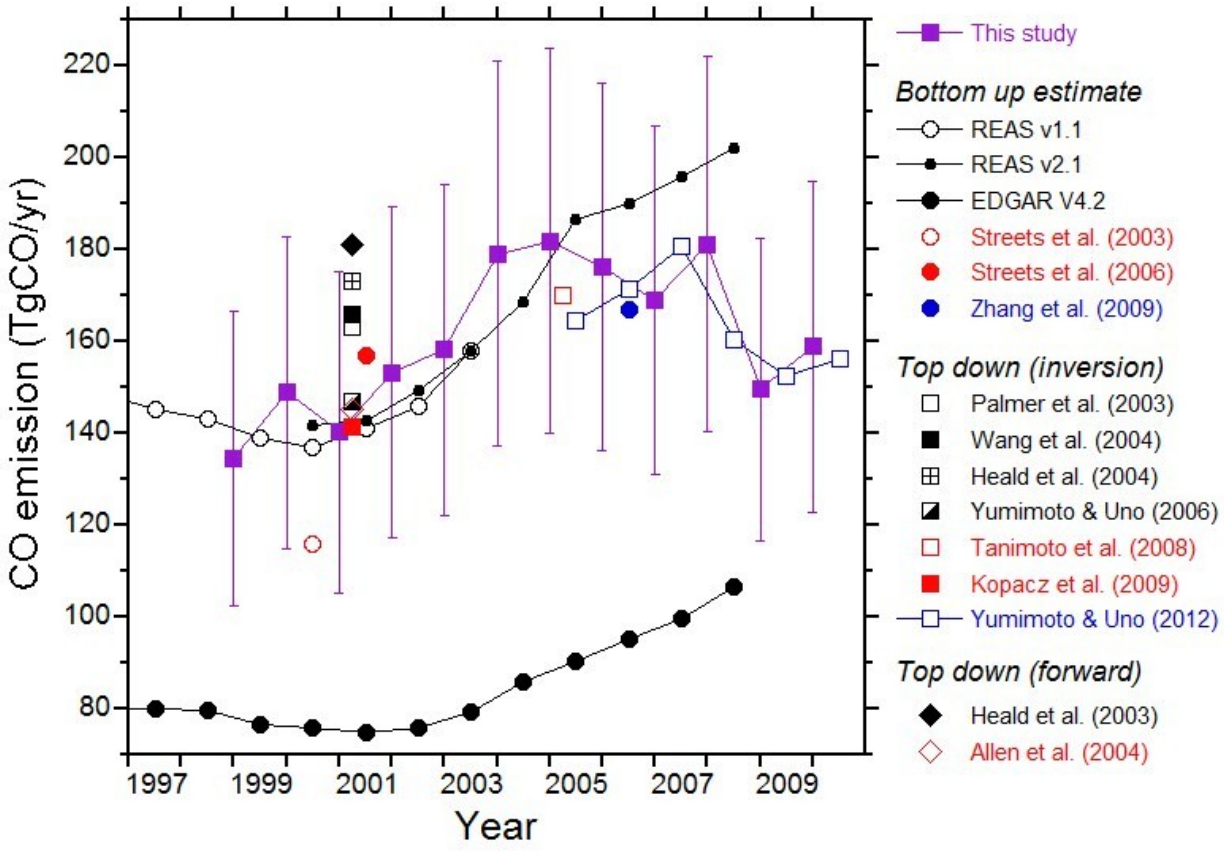

Fig. 10. Comparison of estimated CO emissions from China. The values are expressed as annual emissions. Closed blue squares are the estimated emissions of this study. Circles, squares, and diamonds represent the bottom up estimates, top down (inversion), and top down (forward) estimates, respectively.

Supplementary material

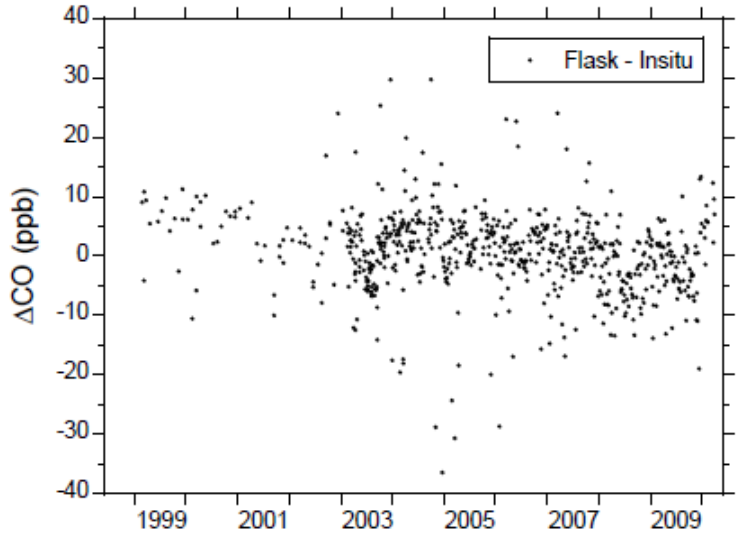

Fig. S1. Time series of the differences between flask and in-situ measurements of the atmospheric CO mixing ratios at HAT during the period from 1999 to 2010.

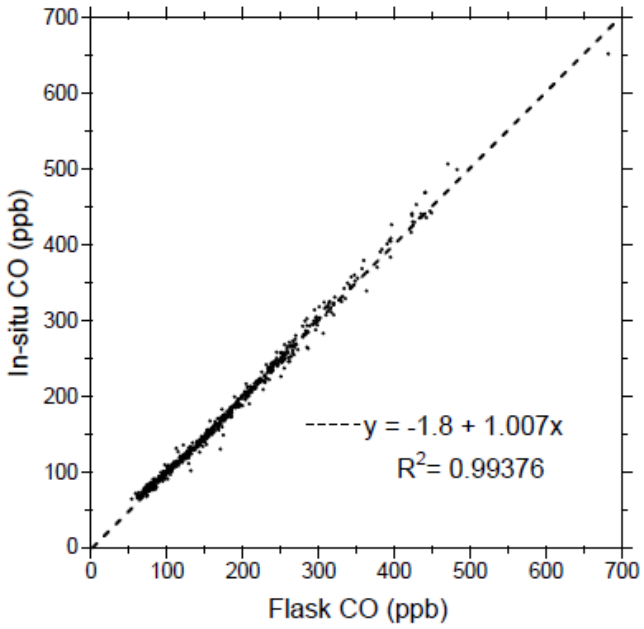

Fig. S2. Scatter plot of the flask and in-situ CO measurements. The broken line represents the linear regression line.

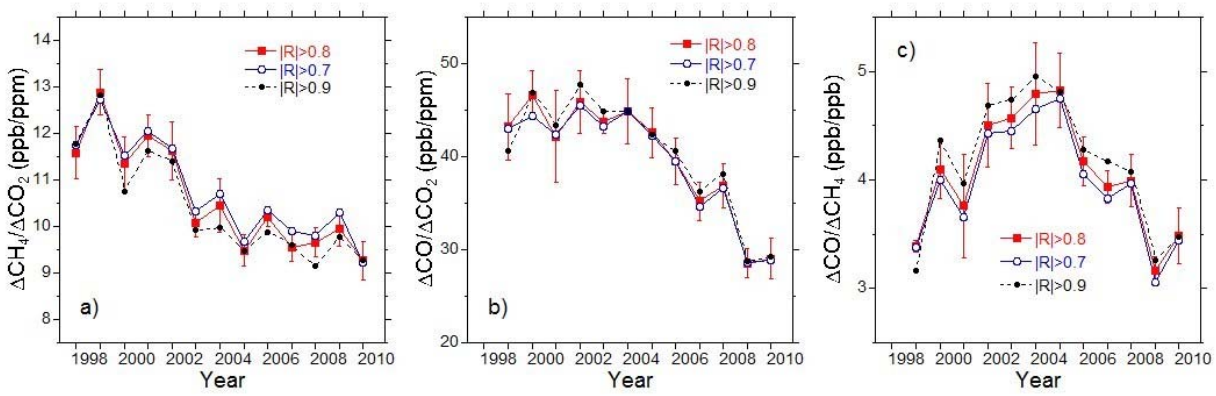

Fig. S3. Temporal changes in the winter average correlation slopes of (a) $\Delta CH_4/\Delta CO_2$, (b) $\Delta CO/\Delta CO_2$, and (c) $\Delta CO/\Delta CH_4$ for 3 correlation coefficients that are used in the selection criteria (see text). The red squares represent the correlation coefficient of 0.8, black open circle 0.7, and black closed circle 0.9.

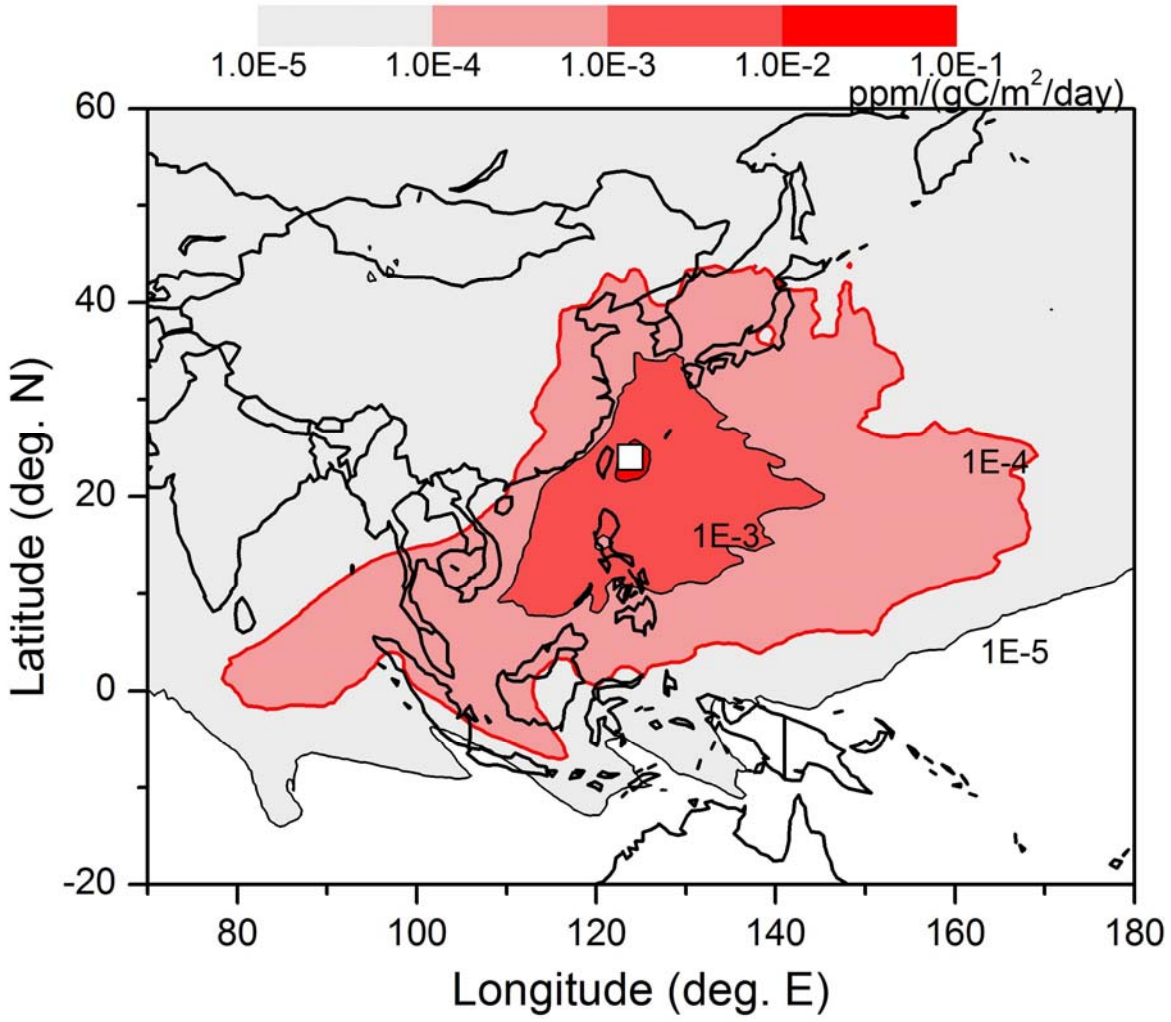

Fig. S4. Average footprint (ppm (gC m^{-2} day^{-1})$^{-1}$) for the measurements at HAT during the summer period (May to September). Meteorological data for 2006-2010 are used for the calculation. The location of HAT is indicated by the square.

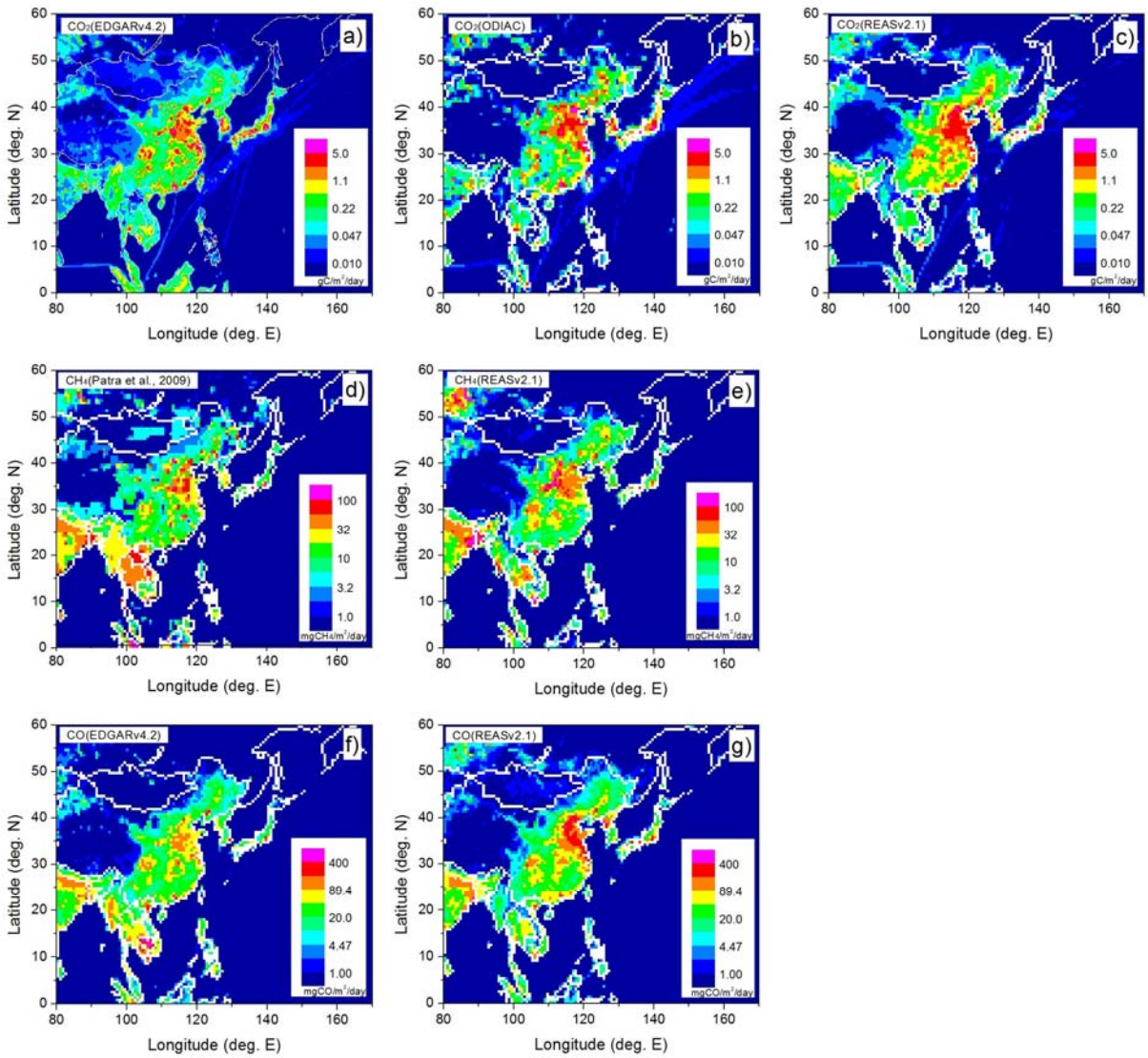

Fig. S5. Comparison of the flux distributions of (a) fossil CO_2 from EDGAR v4.2, (b) fossil CO_2 from ODIAC, (c) fossil CO_2 from REAS v2.1, (d) CH_4 from Patra et al., (2009), (e) CH_4 from REAS v2.1, (f) CO from EDGAR v4.2, and (g) CO from REAS v2.1. The flux maps for 2007 are shown. Annual mean fluxes are depicted for CO_2 and CO, while monthly mean fluxes in January are depicted for CH_4.

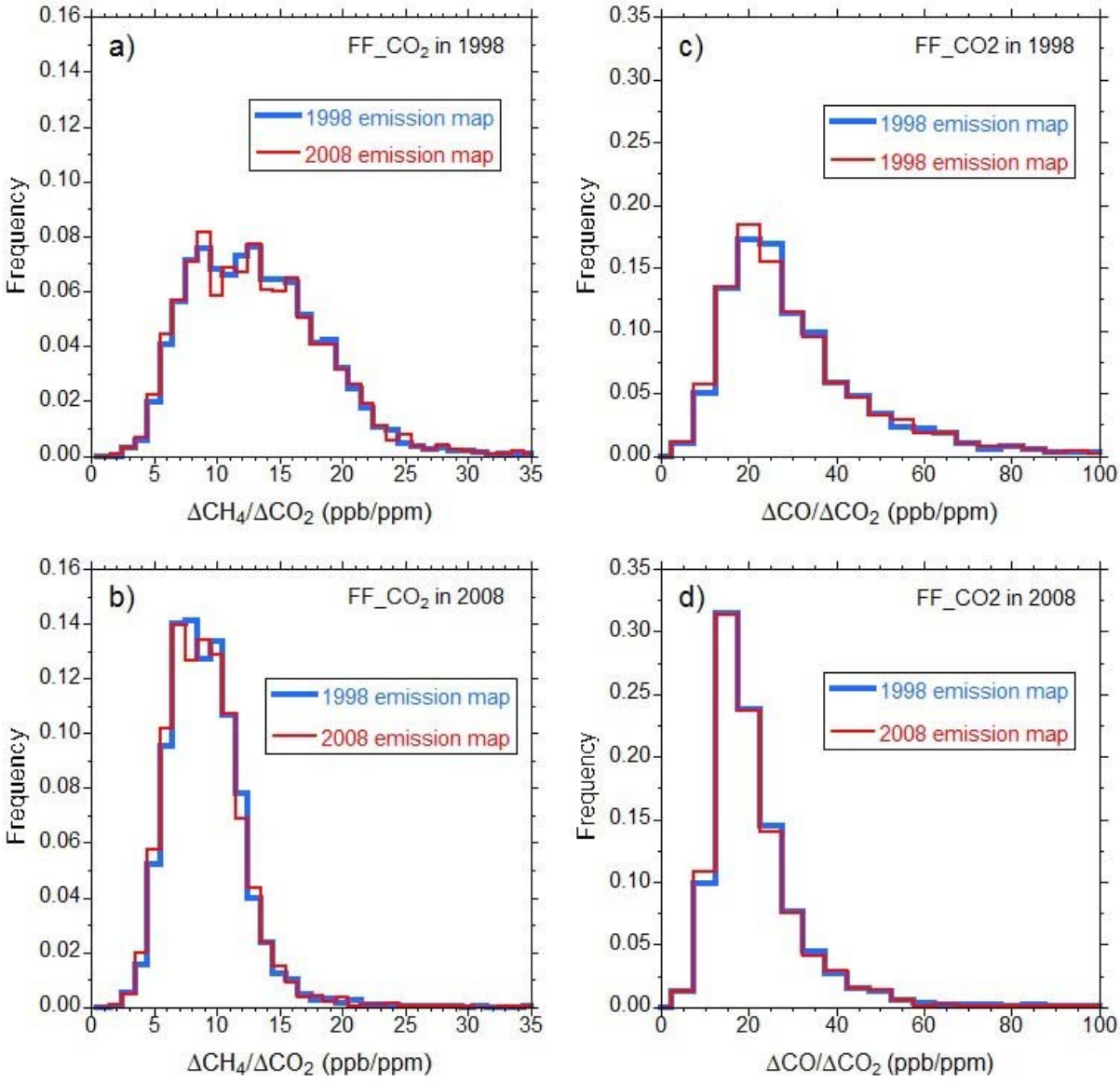

Fig. S6. Histograms of the simulated correlation slopes of (a, b) $\Delta CH_4/\Delta CO_2$ and (c, d) $\Delta CO/\Delta CO_2$ for fossil CO_2 emissions in (a, c) 1998 and (b, d) 2008. The correlation slopes all meet the selection criteria ($|R|>0.8$). The simulated results based on the fossil fuel-derived CO_2 emission maps for 1998 and 2008 are depicted as blue and red lines, respectively.

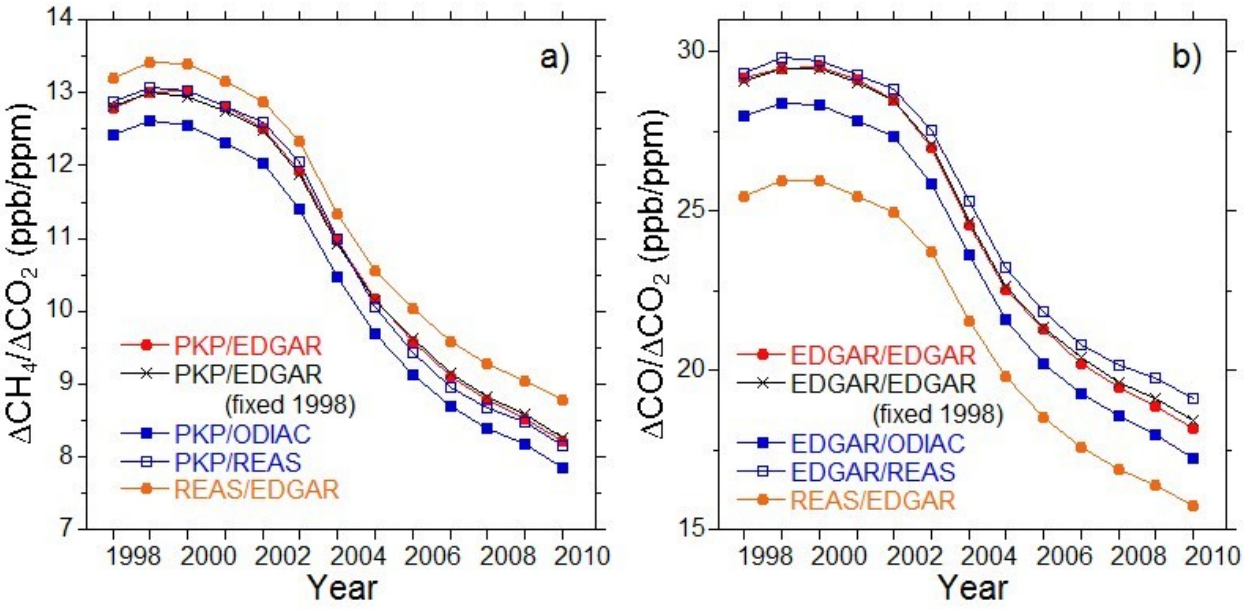

Fig. S7. Comparison of the winter average correlation slopes of simulated (a) $\Delta CH_4/\Delta CO_2$ and (b) $\Delta CO/\Delta CO_2$ for different combinations of the emission maps described in the legend. PKP in the legend represents the CH_4 emissions from Patra et al., (2009). The simulated correlation slopes for the 1998 EDGAR CO_2 emission map are also depicted as crosses.